Heme oxygenase-1–derived carbon monoxide enhances the host defense response to microbial sepsis in mice

Su Wol Chung, Xiaoli Liu, Alvaro A. Macias, Rebecca M. Baron, and Mark A. Perrella

Division of Pulmonary and Critical Care Medicine, Department of Medicine, Brigham and Women's Hospital and Harvard Medical School, Boston, Massachusetts, USA.

Sepsis is characterized by a systemic response to severe infection. Although the inflammatory phase of sepsis helps eradicate the infection, it can have detrimental consequences if left unchecked. Therapy directed against inflammatory mediators of sepsis has shown little success and has the potential to impair innate antimicrobial defenses. Heme oxygenase-1 (HO-1) and the product of its enzymatic reaction, CO, have beneficial antiinflammatory properties, but little is known about their effects on microbial sepsis. Here, we have demonstrated that during microbial sepsis, HO-1–derived CO plays an important role in the antimicrobial process without inhibiting the inflammatory response. HO-1–deficient mice suffered exaggerated lethality from polymicrobial sepsis. Targeting HO-1 to SMCs and myofibroblasts of blood vessels and bowel ameliorated sepsis-induced death associated with *Enterococcus faecalis*, but not *Escherichia coli*, infection. The increase in HO-1 expression did not suppress circulating inflammatory cells or their accumulation at the site of injury but did enhance bacterial clearance by increasing phagocytosis and the endogenous antimicrobial response. Furthermore, injection of a CO-releasing molecule into WT mice increased phagocytosis and rescued HO-1–deficient mice from sepsis-induced lethality. These data advocate HO-1–derived CO as an important mediator of the host defense response to sepsis and suggest CO administration as a possible treatment for the disease.

Introduction

Sepsis represents a complex process of cellular events induced by a severe underlying infection (1, 2). Sepsis has been defined clinically as a syndrome characterized by both the presence of infection and a systemic inflammatory response (3). The invading microorganisms activate immune cells, resulting in the production of proinflammatory mediators that trigger cellular defense mechanisms to fight the infection (4, 5). If therapy is not initiated early (6–9) and the pathogen is not eradicated, organ dysfunction will ensue, followed by refractory hypotension and circulatory failure, which frequently leads to death. Until the late 1980s, sepsis was considered by many to be near synonymous with Gram-negative endotoxemia. More recently, it has become obvious that sepsis can arise from microbial infections in the absence of endotoxin (2). Interestingly, the incidence of Gram-negative sepsis has diminished over the years, and the incidence of Gram-positive and polymicrobial infections now accounts for a high percentage of sepsis cases (9).

Remarkable advances have been made in recent years characterizing the role of the host in the pathobiology of sepsis, from pathogen recognition to the host response to infecting organism(s). Much attention has been placed on TLRs and the molecular signaling pathways in response to microbial pathogens (7, 9–11). TLR4, an essential receptor for lipopolysaccharide recognition in the Gram-negative pathway, has been a particular focus of investigation (12). Beyond TLRs, members of the NACHT-LRR family, which include the nucleotide-binding oligomerization domain (NOD) proteins, recognize peptidoglycans (PGNs) of bacterial cell walls (11). These proteins are expressed mainly in antigen-presenting cells and epithelial cells, including intestinal epithelial cells and Paneth cells (11, 13). NOD2 is able to recognize PGNs from both Gram-positive and Gram-negative bacteria, while NOD1 predominantly senses products of Gram-negative bacteria. Kobayashi and colleagues recently revealed that NOD2 null mice are susceptible to infection by Gram-positive *Listeria monocytogenes* bacteria and NOD2 is required for the expression of intestinal antimicrobial peptides, known as cryptdins/α-defensins (14). These studies confirmed the critical importance of NOD2 in the immune response to microbes within the intestine.

Heme oxygenase-1 (HO-1) is a cytoprotective enzyme that plays a critical role in defending the body against oxidant-induced injury during inflammatory processes (15–17). HO catalyzes the first and rate-limiting step in the oxidative degradation of heme to CO, biliverdin, and ferrous iron (18–20). Biliverdin is converted to bilirubin, a potent endogenous antioxidant (21) with recently recognized antiinflammatory properties (22). CO has numerous biological functions, including antiinflammatory properties (23). In purely inflammatory models of disease, such as endotoxin exposure, HO-1–deficient mice are susceptible to oxidant-induced tissue injury and death (15–17). In contrast, administration of CO or biliverdin/bilirubin to animals exposed to endotoxin decreases inflammation and attenuates end-organ injury (20, 24–27). These studies support the beneficial effects of HO-1 and its products during purely inflammatory processes. Recently, it has also been reported that biliverdin can decrease inflammation during polymicrobial sepsis (28). However, inhibition of the inflammatory response to infection could disrupt the ability of the immune system to eliminate an invading pathogen; thus, questions remain

Nonstandard abbreviations used: ACLP, aortic carboxypeptidase-like protein; CLP, cecal ligation and puncture; CO-RM, CO-releasing molecule; hHO-1, human HO-1; HO, heme oxygenase; NOD, nucleotide-binding oligomerization domain; PGN, peptidoglycan; PMN, polymorphonuclear cell.

Conflict of interest: The authors have declared that no conflict of interest exists.

Citation for this article: *J. Clin. Invest.* **118**:239–247 (2008). doi:10.1172/JCI32730.

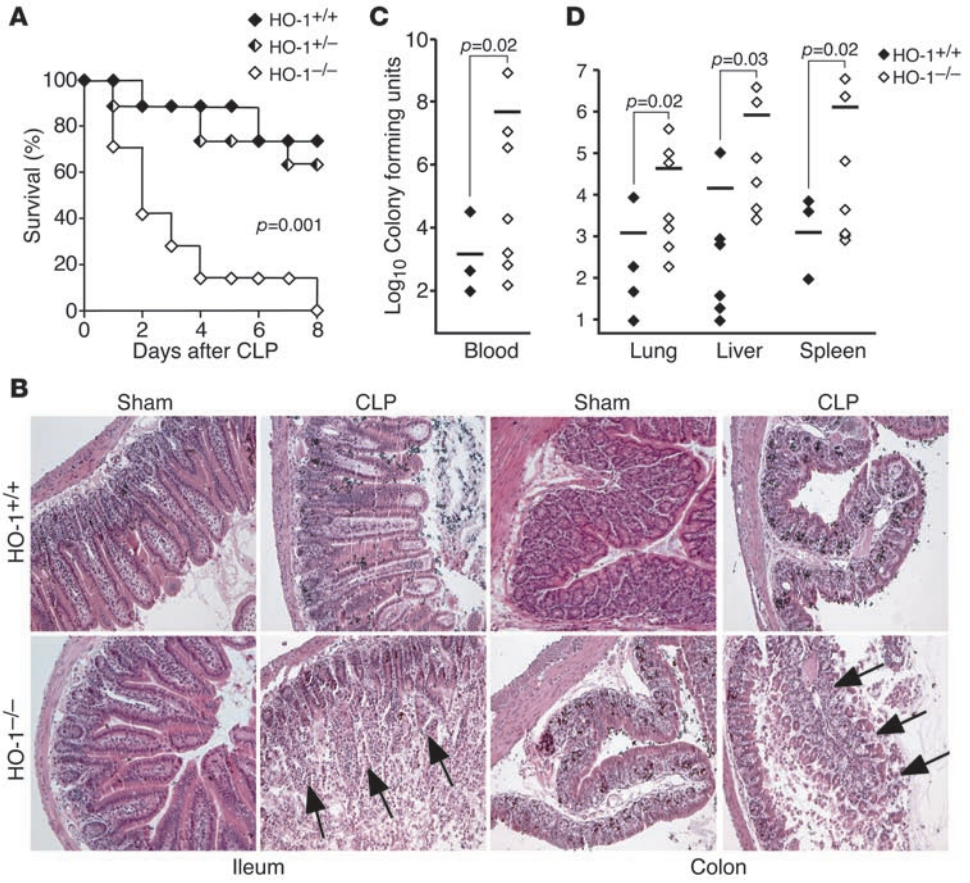

Figure 1
Deficiency of endogenous HO-1 leads to reduced survival after CLP-induced polymicrobial sepsis. (**A**) Rates of survival were determined for HO-1$^{+/+}$ (n = 7), HO-1$^{+/-}$ (n = 8), and HO-1$^{-/-}$ (n = 8) littermates after CLP surgery. P = 0.001. These data are the composite of 3 independent experiments. (**B**) H&E staining of representative paraffin-embedded ileum and colon sections of HO-1$^{+/+}$ and HO-1$^{-/-}$ mice 48 hours after sham or CLP surgery. Original magnification, ×100. Arrows depict destruction of the ileal villi and colonic mucosa. During the first 48 hours after CLP, blood was collected from the right atrium of hearts (**C**), and organs (lungs, livers, and spleens) were homogenized with 1 ml PBS (**D**). Serial dilutions were made of blood and organ homogenates and then plated on LB agar plates. CFUs were determined after incubating at 37°C overnight. Blood: HO-1$^{+/+}$, n = 14; HO-1$^{-/-}$, n = 13. Organs: HO-1$^{+/+}$, n = 9; HO-1$^{-/-}$, n = 8. Horizontal bars represent mean values. These experiments were performed independently 3 times.

regarding the role of HO-1 and the therapeutic potential of CO in microbial sepsis.

Results

Enhanced susceptibility of HO-1 null mice to polymicrobial infection. We performed cecal ligation and puncture (CLP) (19 gauge, 1 hole unless otherwise stated) in WT (HO-1$^{+/+}$), heterozygous (HO-1$^{+/-}$), and HO-1 null (HO-1$^{-/-}$) littermate mice on a pure BALB/c genetic background to induce polymicrobial peritonitis, bacteremia, and sepsis. HO-1$^{-/-}$ mice suffered markedly higher mortality rates compared with HO-1$^{+/+}$ and HO-1$^{+/-}$ mice after CLP-induced sepsis (Figure 1A). While CLP led to an infiltration of inflammatory cells and edema in the villi of the ileum and the submucosal region of the colon in HO-1$^{+/+}$ mice, HO-1$^{-/-}$ mice experienced complete destruction of ileal villi and the mucosal surface of the colon (Figure 1B). Blood was cultured from HO-1$^{+/+}$ and HO-1$^{-/-}$ mice during the first 48 hours after CLP, and CFUs of bacteria were assessed to determine the level of bacteremia. Compared with HO-1$^{+/+}$ mice, circulating levels of bacteria were significantly greater in HO-1$^{-/-}$ mice (Figure 1C). Analogous to cultures of blood, organ homogenates (lungs, livers, and spleens) from HO-1$^{-/-}$ mice showed significantly higher levels of bacteria than HO-1$^{+/+}$ mice (Figure 1D). Thus, in the absence of HO-1, CLP-induced sepsis leads to a destructive process in the ileum and colon and increased bacteremia, resulting in end-organ seeding. These data demonstrate the importance of endogenous HO-1 in protecting mice against the lethal effects of polymicrobial sepsis.

Overexpression of HO-1 has beneficial effects during polymicrobial sepsis. Due to the detrimental effects of HO-1 deficiency, we hypothesized that targeted overexpression of HO-1 would be beneficial during microbial-induced sepsis. Since the route of infectious dissemination in sepsis is the bloodstream, we overexpressed HO-1 in the vasculature. Tg mice on a pure C57BL/6 background were generated using the promoter of aortic carboxypeptidase-like protein (ACLP) (29) to target human HO-1 (hHO-1) in vascular SMCs. ACLP is able to target Tg expression not only in large-sized and medium-sized vessels but also in small vessels down to the arteriole (29). The Tg construct is shown in Figure 2A. The founder mice

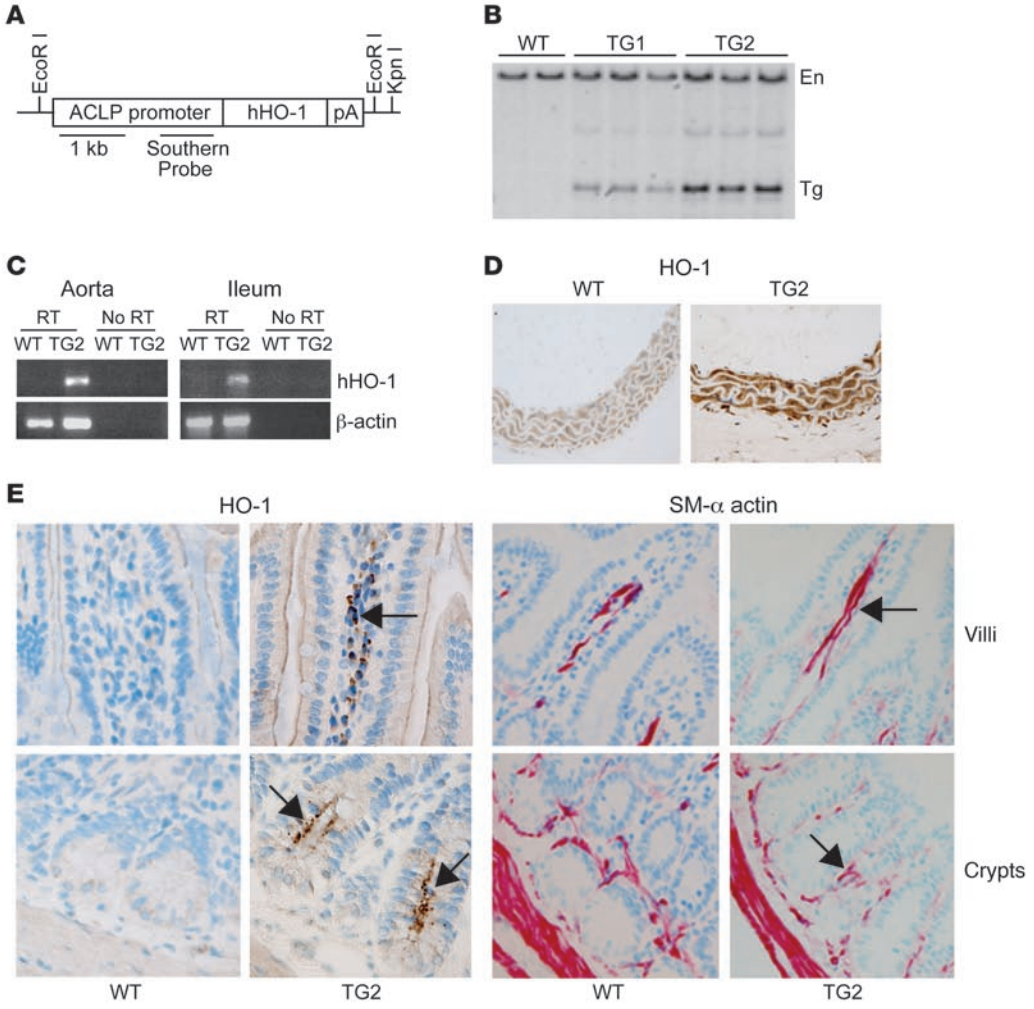

Figure 2

Generation and characterization of HO-1 Tg mice. (**A**) Schematic of the Tg construct. ACLP promoter indicates 2.5 kb of the ACLP promoter known to express in SMCs. hHO-1, 1-kb hHO-1 cDNA; pA, 300-bp bovine growth hormone polyadenylation sequences. The position of the Southern probe is shown below the construct. (**B**) Southern blot analysis of EcoRI-digested genomic DNA from WT and Tg1 and Tg2 Tg mice is shown. En, endogenous. (**C**) Total RNA was isolated from aortas of WT and Tg2 mice, and RT-PCR performed using hHO-1–specific primers. Mouse β-actin was used as an internal positive control for the PCR reaction, and "No RT" indicates the negative control. Sections from aortas (**D**) and villi and crypts of the ileum (**E**) from WT and Tg2 mice were stained with HO-1 antiserum. Sections from ileum were also stained with antiserum against smooth muscle (SM) α-actin. Brown staining indicates HO-1 expression (**D**, 4 left panels of **E**), and red staining indicates smooth muscle α-actin expression (4 right panels of **E**). Original magnification, ×100 (**D** and **E**). Arrows depict HO-1 and smooth muscle α-actin–expressing cells in villi and crypts of the ileum and colon, respectively.

were identified by Southern blot analysis of genomic DNA (Figure 2B), and we obtained mice with either 1 (Tg1) or 2 (Tg2) copies of the Tg. To confirm mRNA expression of the Tg, total RNA was isolated from aortas of WT and Tg2 mice and RT-PCR performed using hHO-1–specific primers. The hHO-1 Tg was only present in the Tg mice (Figure 2C). Also, the level of HO-1 protein expression was detected in the aortas of Tg2 mice by immunostaining and compared with expression in WT mice (Figure 2D). We found that the expression of HO-1 protein was significantly increased, by 3.5-fold, in the vasculature of Tg2 mice compared with WT mice (n = 3 in each group; P = 0.0034) by colorimetric analysis as described previously (30, 31).

HO-1–derived CO is known to exhibit biologic effects, including the modulation of vascular tone (32) and the inhibition of inflammatory signaling, by suppressing proinflammatory cytokines (TNF-α and IL-1β) and upregulating the antiinflammatory cytokine IL-10 (24). Since hypotension and the systemic inflammatory response are critical contributors to the morbidity and mortality of sepsis, we assessed baseline systolic blood pressure, as described previously (17), and levels of circulating cytokines. Tg2 mice showed comparable baseline blood pressures (Supplemental Figure 1A; supplemental material available online with this article; doi:10.1172/JCI32730DS1) and no difference in circulating levels of proinflammatory (TNF-α, IL-1β, IL-6) and antiinflammatory (IL-10) cytokines compared with WT mice (Supplemental Figure 1B).

With evidence that baseline blood pressure and inflammatory cytokine production was comparable, we next wanted to determine whether vascular overexpression of HO-1 would improve outcome

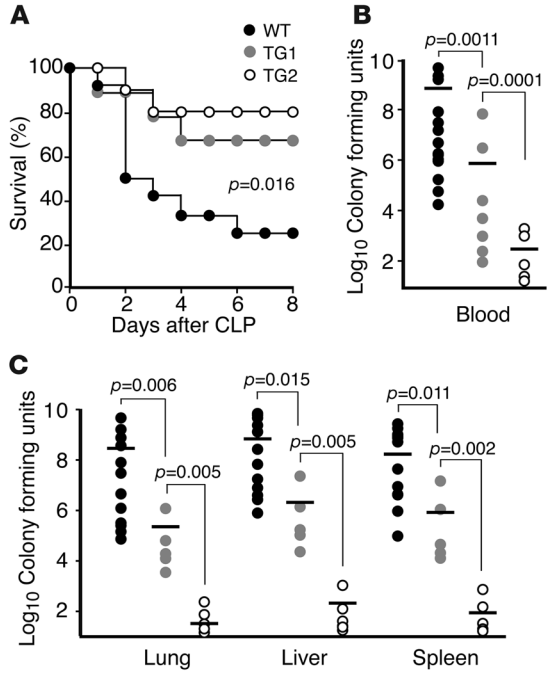

Figure 3
Improved survival from polymicrobial sepsis in HO-1 Tg mice. (**A**) Survival was assessed in HO-1 Tg (Tg1, $n = 9$; Tg2, $n = 10$) and WT ($n = 12$) mice after CLP-induced polymicrobial sepsis. $P = 0.016$. These data are a composite from 2 independent experiments. Analogous to what was reported in Figure 1, blood was collected from the right atrium of hearts (**B**), and organs (lungs, livers, and spleens) were homogenized (**C**) from WT, Tg1, and Tg2 mice. Serial dilutions were made of blood and organ homogenates, and CFUs were determined after incubating at 37°C overnight on LB agar plates. Blood: WT, $n = 12$; Tg2, $n = 8$. Organs: WT, $n = 8$; Tg2, $n = 6$. Horizontal bars represent mean values. These experiments were performed independently at least 2 times.

in polymicrobial sepsis. Thus, Tg mice (Tg1 and Tg2) and WT mice on a pure C57BL/6 background underwent CLP. Note that survival rate of WT mice after 19-gauge, 1-hole CLP is lower on a C57BL/6 compared with a BALB/c genetic background (see Methods). Both Tg1 and Tg2 mice demonstrated significantly improved survival after CLP compared with WT mice (Figure 3A). Bowel histopathology after CLP surgery showed similar tissue injury in the ileum of WT, Tg1, and Tg2 mice, with evidence of inflammation and villi shortening (Supplemental Figure 2). In the colon, a greater amount of submucosal edema was noted in the WT mice (Supplemental Figure 2) compared with Tg1 and Tg2 mice. However, in contrast to HO-1$^{-/-}$ mice, there was no evidence of gross tissue destruction in the ileum or colon of WT, Tg1, or Tg2 mice. To help elucidate why mortality was different among the groups, we performed blood cultures in WT, Tg1, and Tg2 mice. Tg1 mice had significantly lower bacterial counts in the circulating blood than WT mice, and the decrease in bacterial counts was even more pronounced in Tg2 mice compared with either WT or Tg1 mice (Figure 3B). Lower bacterial counts were also seen in end-organ cultures from lungs, livers, and spleens of Tg mice compared with WT mice (Figure 3C). Similar to the circulating blood, bacterial counts in the end organs decreased in a dose-dependent fashion depending on the copy number of HO-1 Tgs. These data suggest that, beyond protecting bowel integrity, vascular overexpression of HO-1 has a more direct antimicrobial effect during CLP-induced polymicrobial sepsis. Due to the similarity in survival response to CLP in Tg lines, we focused on the Tg2 mice for the remainder of the experiments.

Overexpression of HO-1 has beneficial effects against Gram-positive Enterococcus faecalis–induced sepsis. Because of the mixed bacterial flora of CLP-induced sepsis, we wanted to know whether overexpression of HO-1 would have a different effect on infection from Gram-positive versus Gram-negative organisms. Aerobic cultures of cecal contents determined that the most prevalent organisms in the bowel were *Enterococcus faecalis* (Gram-stain positive) and *Escherichia coli* (Gram-stain negative) and the bacterial flora did not differ between WT and Tg2 mice (data not shown). To allow a slow and progressive release of microorganisms, similar to the CLP model of polymicrobial sepsis, we used a fibrin clot model of single organism sepsis (33), with placement of the bacterial fibrin clot in the abdominal cavity. Tg2 mice experienced no protection from *E. coli*–induced mortality (Figure 4A); however, overexpression of HO-1 significantly improved survival from *E. faecalis*–induced sepsis in Tg2 mice compared with WT mice (Figure 4B).

HO-1–derived CO increases phagocytic activity of E. faecalis in a NOD2-dependent fashion. With this differential survival in HO-1 Tg mice to *E. faecalis* but not *E. coli* infection, additional studies were performed to determine whether a difference was evident in the ability of inflammatory cells to phagocytize the bacteria. Nonlabeled or FITC-labeled *E. coli* and *E. faecalis* were injected into the peritoneum of WT or Tg2 mice. After 24 hours, a peritoneal lavage was performed and phagocytic rates were determined using flow cytometry as described in Methods. Phagocytosis was not different between WT and Tg2 mice exposed to *E. coli* ($P = 0.462$); however, exposure to *E. faecalis* led to a 48% increase ($P = 0.001$) in phagocytic rate in mice overexpressing HO-1 (Figure 5A). To determine whether there was a difference in the inflammatory response between WT and Tg2 mice, we measured total inflammatory cells/phagocytic cells 24 hours after injection of heat-killed *E. faecalis* into the peritoneum. Flow cytometry analysis revealed that cells were predominantly neutrophils and that the total neutrophil count was not different between WT and Tg2 mice (Figure 5B). Inflammatory cells were also analyzed from the peripheral blood after CLP surgery, and analogous

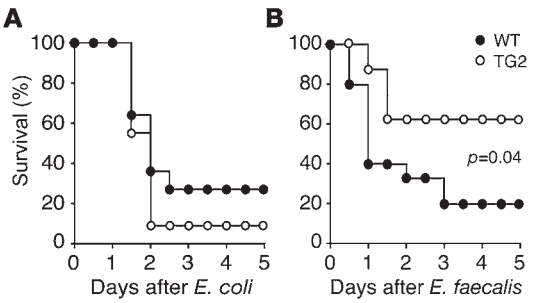

Figure 4
Beneficial effects of HO-1 Tg on Gram-positive but not Gram-negative bacteria. Survival was assessed in Tg2 ($n = 11$) and WT ($n = 11$) mice after fibrin clot–induced microbial sepsis by *E. coli* (3×10^8) bacteria (**A**) and in mice (Tg2, $n = 8$; WT, $n = 15$) receiving *E. faecalis* (2×10^8) bacteria (**B**). $P = 0.04$ for *E. faecalis* and not significant for *E. coli*.

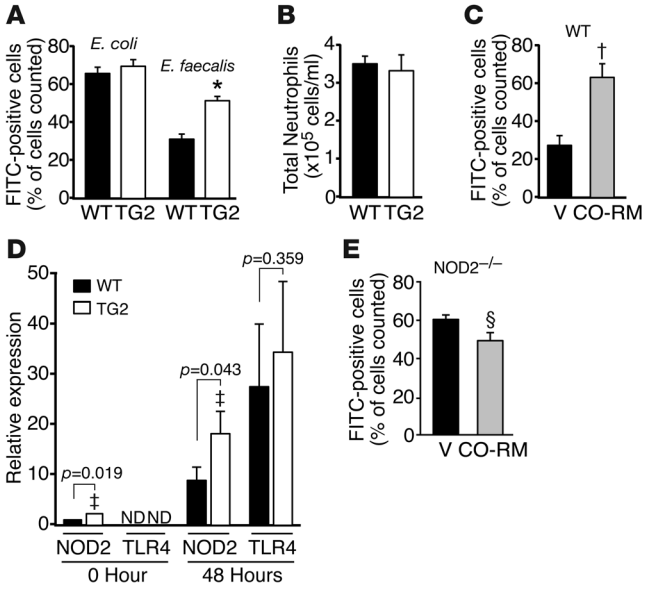

Figure 5
HO-1–derived CO enhances phagocytosis. (**A**) Tg2 ($n = 6$) and WT ($n = 6$) mice were injected with FITC-labeled *E. coli* or *E. faecalis*. After 24 hours, phagocytosis was analyzed. *$P = 0.001$ versus WT. (**B**) Total neutrophil counts were measured 24 hours after injection of nonlabeled *E. faecalis* into Tg2 ($n = 6$) and WT ($n = 7$) mice. (**C**) WT mice were injected with CO-RM (10 μM/kg, $n = 5$) or vehicle (12.5% DMSO, $n = 5$) 12 hours and 2 hours before injection of FITC-labeled *E. faecalis*. After 24 hours, phagocytosis was measured. †$P = 0.004$ versus V. (**D**) NOD2 and TLR4 mRNA levels were quantified by real-time PCR of total ileum RNA isolated at baseline (WT, $n = 5$; Tg2, $n = 4$) and 48 hours after CLP-induced sepsis (WT, $n = 13$; Tg2, $n = 15$). ‡$P = 0.019$ and 0.043 versus WT. (**E**) NOD2$^{-/-}$ mice were injected with CO-RM ($n = 5$) or vehicle ($n = 6$) 12 hours and 2 hours before injection of FITC-labeled *E. faecalis*. After 24 hours, phagocytosis was measured. §$P = 0.038$ versus V. Data are presented as mean ± SEM.

to what is shown in Figure 5B, circulating levels of total inflammatory cells (leukocytes) were not different between WT and Tg2 mice (Supplemental Figure 3A). Moreover, circulating levels of TNF-α, IL-1β, IL-6, and IL-10 were not significantly different between WT and Tg2 mice at 48 hours, a point in time when mortality differences were starting to become apparent between groups (Supplemental Figure 3C). In addition, circulating levels of TNF-α and IL-6 were not different between WT and Tg2 mice 6 hours after CLP surgery (Supplemental Figure 3B). Thus, overexpression of hHO-1 did not change the overall inflammatory response, as judged by circulating inflammatory cells and the production of inflammatory cytokines 6 and 48 hours after CLP, but it did enhance the ability of neutrophils to phagocytize *E. faecalis* bacteria.

ACLP targeting is able to increase hHO-1 expression in SMCs but not inflammatory cells. However, since CO — a product of heme catabolism by HO-1 — is able to diffuse across cell boundaries and exhibit biological functions on neighboring cells (34), we proposed that targeting HO-1 to vascular cells would allow biological actions on adjacent inflammatory cells infiltrating into critical organs during sepsis. To test this hypothesis, we investigated whether CO could enhance the phagocytic properties of inflammatory cells in vivo. CO-releasing molecule (CO-RM) or an equal volume of vehicle was injected into the peritoneum of WT C57BL/6 mice 12 hours and 2 hours before injection of nonlabeled or FITC-labeled *E. faecalis*. Administration of CO-RM to mice promoted a significant increase in the phagocytic rate (2.3-fold; $P = 0.004$) compared with vehicle-treated mice (Figure 5C). The importance of CO in regulating this response, in contrast to another metabolite of HO-1, was confirmed by experiments showing that administration of biliverdin did not enhance the phagocytic response during *E. faecalis* infection (data not shown).

Interestingly, hHO-1 Tg is also expressed in the ileum of Tg mice (Figure 2C) in cells adjacent to intestinal epithelial cells and Paneth cells of the villi and crypts (Figure 2E). These hHO-1–expressing cells also stain positive for smooth muscle α-actin (Figure 2E) and are consistent with myofibroblasts. To further investigate mechanisms by which HO-1 may promote antibacterial effects, we assessed the expression of TLR4 and NOD2 in tissue from the ileum of WT and HO-1 Tg mice. Studies using real-time PCR analyses revealed that baseline NOD2 expression was increased in Tg2 mice compared with WT mice (Figure 5D). Moreover, increased expression of NOD2 after CLP-induced polymicrobial sepsis was enhanced in Tg2 mice compared with WT mice. In contrast, mRNA levels of TLR4 were not detectable at baseline, and after CLP-induced sepsis, the levels of TLR4 were similar between WT and Tg2 mice (Figure 5D).

To elucidate whether enhanced phagocytic activity by CO is related to expression of NOD2, we performed phagocytic assays in

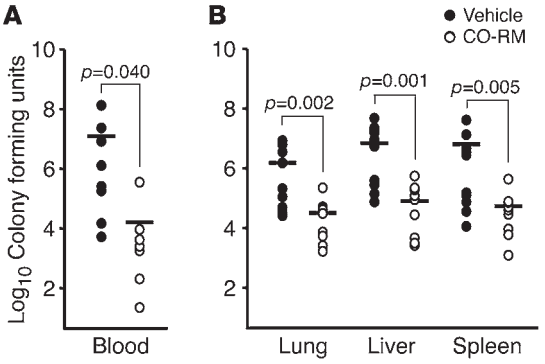

Figure 6
CO-RM enhances bacterial clearance. WT mice were injected with CO-RM ($n = 10$) or vehicle ($n = 10$) 12 hours and 2 hours before CLP surgery. After 24 hours, CFUs were determined from blood (**A**) and organs (**B**). Horizontal bars represent mean values. These experiments were performed independently at least 2 times.

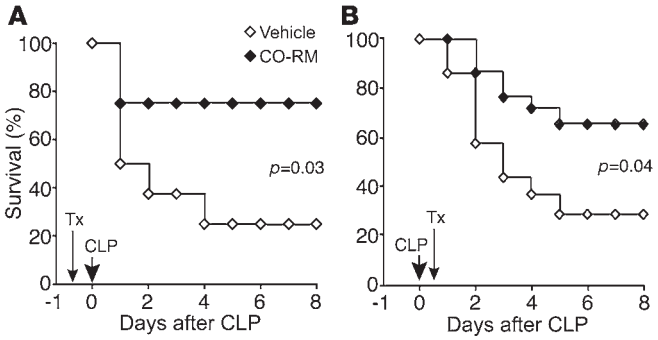

Figure 7
CO-RM rescues mice from the mortality of CLP-induced polymicrobial sepsis. (**A**) Treatment (Tx) with CO-RM (10 μM/kg, n = 8) or an equal volume of vehicle (12.5% DMSO in PBS, n = 8) was administered intraperitoneally to HO-1$^{-/-}$ mice 12 hours and 2 hours before and every 24 hours after CLP surgery (19 gauge, 1 hole). Survival rates were then assessed over the subsequent 8 days. P = 0.03. The data are a composite of 3 independent experiments. (**B**) Treatment with CO-RM (10 μM/kg, n = 14) or an equal volume of vehicle (n = 14) was administered intraperitoneally to HO-1$^{+/+}$ mice starting 6 hours after CLP surgery (19 gauge, 2 holes), after 12 hours, and then every 24 hours. Survival rates were assessed over the subsequent 8 days. P = 0.04. Data are a composite of 5 independent experiments. Short arrows depict the time of CLP surgery, and the longer arrows represent the initiation of treatment, either CO-RM or vehicle.

NOD2$^{-/-}$ mice after administration of CO-RM or vehicle. Beyond ileal tissue, NOD2 was expressed in phagocytic cells from peritoneal lavage of WT mice exposed to heat-killed *E. faecalis* (data not shown). In contrast to the increased phagocytosis in WT mice, NOD2$^{-/-}$ mice exposed to CO-RM demonstrated no evidence of an increase and, in fact, exhibited a modest decrease in phagocytic activity (18.5%) compared with vehicle-treated mice (Figure 5E). These data suggest that expression of NOD2 is critical for enhancing phagocytic activity by CO in inflammatory cells.

CO-RM enhances bacterial clearance during CLP-induced polymicrobial sepsis. With evidence of enhanced phagocytosis by CO-RM, we wanted to determine whether this response resulted in decreased bacteremia. Thus, CO-RM or an equal volume of vehicle was administered intraperitoneally to WT C57BL/6 mice 12 hours and 2 hours prior to CLP surgery. The mice were then sacrificed 24 hours after CLP surgery and bacteremia quantitated. The mice receiving CO-RM had significantly lower circulating bacterial counts (CFUs) than vehicle-treated mice (Figure 6A). The lower bacterial counts in the CO-RM group were also seen in end organs, as shown in cultures from lungs, livers, and spleens (Figure 6B). These data are consistent with decreased bacteremia and end-organ infection in Tg2 mice (Figure 3, B and C).

CO-RM has therapeutic effects and rescues HO-1$^{-/-}$ mice from the increased mortality of CLP-induced polymicrobial sepsis. Our data suggest that CO is a key product of HO-1–derived heme catabolism, contributing to the host defense response during polymicrobial sepsis. We next administered CO-RM or vehicle to HO-1$^{-/-}$ mice 12 hours and 2 hours prior to CLP surgery and every 24 hours after the initiation of sepsis. CO-RM administration to HO-1$^{-/-}$ mice resulted in significantly improved survival compared with vehicle-treated HO-1$^{-/-}$ mice (Figure 7A). These data demonstrated that CO can rescue HO-1$^{-/-}$ mice from the detrimental outcome of CLP-induced sepsis and verified the critical importance of CO in the microbial response to sepsis. To determine the therapeutic potential of CO, we administered CO-RM to WT BALB/c mice starting 6 hours after CLP surgery (19 gauge, 2 holes). At this point in time, bacteria have already begun to seed end organs (data not shown). As revealed in Figure 7B, CO-RM is able to significantly improve survival from CLP surgery, even when administered after the onset of sepsis.

Discussion

Sepsis is the leading cause of death in critically ill patients in the United States (1), and the incidence of sepsis continues to rise (35, 36). Thus, it is critical for investigators to continue to explore the pathophysiologic basis of sepsis in an effort to consider new therapeutic options. The present study demonstrates the importance of endogenous HO-1 expression in protecting against the lethal effects of polymicrobial sepsis (Figure 1). The gross tissue destruction and loss of bowel integrity in the ileum and colon of HO-1$^{-/-}$ mice allowed us to identify a causative reason for exaggerated death in these mice. However, WT and Tg mice overexpressing HO-1 did not experience this level of tissue injury (Supplemental Figure 2), which is more consistent with autopsy findings of human patients with sepsis whose histologic findings often do not reflect the severity of organ dysfunction (37). Since HO-1 is known to play an important antiinflammatory role in response to injurious stimuli (18–20), we also investigated the inflammatory response during CLP-induced peritonitis and sepsis in mice overexpressing HO-1 to help explain the improved survival. Infiltration of inflammatory cells into the peritoneum did not differ between WT and Tg2 mice in terms of overall cell number (Figure 5B), yet Tg2 mice demonstrated increased phagocytosis of *E. faecalis* (Figure 5A). This difference in phagocytic rate corresponded with less susceptibility to *E. faecalis*–induced death in Tg2 mice (Figure 4B). We also demonstrated that administration of CO-RM enhanced phagocytosis of *E. faecalis* in vivo (Figure 5C). Otterbein and colleagues have shown in vitro that CO increased macrophage phagocytosis of *E. coli* in the RAW 264.7 cell line (38). However, when assessing the neutrophil response in vivo, Tg2 mice did not demonstrate an increased phagocytic response to *E. coli* (Figure 5A).

Nakahira and colleagues recently reported that CO inhibited signaling of TLR pathways, including TLR4 as well as TLR2, -5, and -9 (39). This inhibition of signaling produced a decrease in the production of proinflammatory cytokines, such as TNF-α, in macrophages. While reduced production of proinflammatory cytokines is critical for resolving inflammatory-driven insults like endotoxemia, the question remains whether the suppression of an inflammatory response by CO could alter the ability of the immune system to eliminate an invading pathogen. Our studies do not suggest a problem in eradicating bacterial pathogens, and in fact, CO enhanced phagocytosis of *E. faecalis* by neutrophils (Figure 5C) and decreased bacteremia and end-organ seeding in CLP-induced sepsis in mice (Figure 6, A and B).

We witnessed no difference in TLR4 expression in our mice; thus, we focused our efforts on NOD2 and its regulation by HO-1. This decision was also based on the fact that NOD2 recognizes PGNs from most bacteria, including Gram-positive organisms (11, 13), and that NOD2 plays a significant role in the intestinal immune response. Moreover, recent evidence suggests that in the absence of NOD2, mice are susceptible to infection in the

gastrointestinal tract by the Gram-positive organism *L. monocytogenes* (14). The increased expression of NOD2 in HO-1 Tg mice, not only after CLP-induced sepsis but also at baseline (Figure 5D), may have important implications, as NOD2 contributes to the maintenance of commensal mucosal homeostasis in the bowel and prevents intracellular invasion of bacteria (40). The importance of NOD2 in intestinal immunity, both for surveillance purposes and for controlling bacterial pathogens, is underscored by the fact that genetic mutations in the NOD2 gene have been associated with the development of autoimmune diseases in humans, such as Crohn disease (11). Interestingly, we also demonstrated that the CO-RM–induced increase in phagocytosis by inflammatory cells was lost in the absence of NOD2 (Figure 5E). We propose that, in conjunction with an enhanced phagocytic response, NOD2 expression is critical for the improved outcome in mice overexpressing HO-1 or receiving CO-RM during a microbial insult.

Our studies suggest that HO-1–derived CO is able to diffuse across cell boundaries and exhibit biological functions on adjacent cells, as shown by the increased phagocytosis of *E. faecalis* by inflammatory cells in Tg mice overexpressing HO-1 in the vascular wall (Figure 5A). This ability of HO-1–derived CO to exhibit biological functions on adjacent cells has been demonstrated previously in vivo, as Tg mice overexpressing HO-1 in lung alveolar epithelial cells are able to prevent hypoxia-induced pulmonary hypertension, vascular remodeling, and pulmonary inflammation (34). In support of this concept, administration of CO-RM was able to increase phagocytosis, decrease circulating bacterial counts, and rescue HO-1$^{-/-}$ mice from the exaggerated mortality of CLP-induced sepsis (Figure 7A). While functional polymorphisms in the HO-1 promoter have been shown to predispose patients to vascular disease (41), an absolute deficiency in HO-1 is uncommon in humans (42). Thus, to assess the therapeutic potential of CO, we administered CO-RM to WT mice after the inception of sepsis. This is critical, as sepsis is diagnosed and therapy initiated after the onset of the clinical syndrome. When administered 6 hours after the onset of sepsis, a point in time at which organ dysfunction has begun after CLP surgery (43) and bacteria have already seeded end organs (lung, liver, spleen), CO-RM was able to improve survival in a model of abdominal sepsis (Figure 7B).

The present study provides what we believe is novel information regarding the ability of HO-1 to improve the ability of inflammatory cells to phagocytize bacteria during abdominal sepsis, with a more selective response for Gram-positive *E. faecalis*. While HO-1 and CO are known to have antiinflammatory properties in pure inflammatory models of disease, during a microbial model of sepsis, HO-1 did not suppress circulating inflammatory cells or their accumulation at the site of injury and HO-1 did not suppress circulating proinflammatory cytokines during early (6 hours) or late (48 hours) time points after bowel injury. This combination of properties, controlling infection without producing an immunosuppressive environment, allowed the eradication of bacteria and improved survival. Also, we demonstrate for what we believe is the first time that the improved phagocytic response by HO-1, and subsequently CO, is dependent on NOD2 expression. These beneficial effects of CO promote improved survival even when administered 6 hours after the onset of polymicrobial sepsis. Thus, our study provides additional insight into the pathophysiology of sepsis and underscores the valuable properties of HO-1 during a systemic microbial process.

Methods

Reagents. CO-RMs are transition metal carbonyls, which liberate CO to elicit direct biological activities (44). These compounds are able to release CO in a concentration-dependent manner. The CO-RM used in our experiments was tricarbonyldichlororuthenium (II) dimmer ($[Ru(CO)_3Cl_2]_2$) (Sigma-Aldrich).

CLP model of polymicrobial sepsis. Animal care and use for all experiments was approved by the Harvard Medical Area Standing Committee on Animals, Harvard Medical School. The CLP model of polymicrobial sepsis was performed as previously described (45). Anesthesia was induced in mice by intraperitoneal administration of 100 mg/kg ketamine HCl and 43 mg/kg xylazine HCl. The mouse cecum was exposed through a 1.5-cm incision and the cecum ligated below the ileocecal valve with a 6-0 silk suture without causing bowel obstruction and then punctured through with a 19-gauge needle. A 19-gauge, 1 hole injury was performed in studies using HO-1 null and HO-1 Tg mice on a BALB/c and C57BL/6 background, respectively. The cecum was repositioned, and the abdominal incision was closed in layers with 6-0 surgical sutures (Harvard Apparatus). Sham-operated mice underwent the same procedure, including opening of the peritoneum and exposing the bowel, but without ligation and needle perforation of the cecum. After surgery, the mice were injected with 1 ml of physiologic saline solution subcutaneously for fluid resuscitation. No antibiotics were administered to the mice after CLP, as we wanted to assess the effect of HO-1 and CO-RM on bacterial levels in the blood and organs. Survival rates were determined over an 8-day period, with assessment every 12 hours. Pre- and postoperatively, all mice had unlimited access to food and water.

Genetic background of mice and CLP. Severity of disease in the CLP model varies by genetic background (46). CLP-induced mortality is worse in WT mice of C57BL/6 background (Figure 3A) compared with BALB/c background (Figure 1A), using 19-gauge, 1-hole injury. Injury of 19 gauge, 1 hole in C57BL/6 mice is similar to 19-gauge, 2-hole injury in BALB/c mice (Figure 7B).

Gene-deficient mice. HO-1$^{-/-}$ mice were generated as described (16), and bred back to a pure BALB/c genetic background. NOD2$^{-/-}$ mice were obtained from The Jackson Laboratory on a pure C57BL/6 genetic background.

Generation of Tg construct. To generate a Tg construct (Figure 2A) expressing the hHO-1 cDNA under the control of ACLP promoter, a 300-bp DNA fragment containing bovine growth hormone polyadenylation sequences (bGHpA) was ligated 3′ to the 1 kb hHO-1 cDNA open-reading frame. The fragment containing hHO-1/bGHpA was then ligated downstream from 2.5 kb of the mouse ACLP promoter. A 4.0-kb *SacI-KpnI* DNA fragment was isolated, purified, and injected into the pronuclei of fertilized C57BL/6 mouse eggs (Brigham and Women's Hospital, Core Transgenic Mouse Facility). Tg mice harboring the ACLP promoter/hHO-1 cDNA were identified by Southern blot analysis with genomic DNA prepared from tail biopsies using ACLP promoter probe. To determine the Tg copy number, Southern blot analysis was performed with EcoRI digested genomic DNA and a ^{32}P-labeled 1.0-kb *EcoRI* ACLP fragment as a probe (Figure 2B) that recognized an endogenous fragment (En) and a Tg fragment. Radioactivity was measured on a PhosphorImager running ImageQuant software (Molecular Dynamics). Tg copy number was determined by first calculating the ratio of the Tg/En bands and then multiplying by a factor of 2 (for the 2 endogenous copies). Mice were used at 8–12 weeks of age.

Bacteria culture from blood and tissues. The mice were sacrificed under anesthesia, and blood was collected from the right atrium of the heart; lung (left), liver (left medial lobe), and whole spleen were harvested and ground with 1 ml of PBS. Serial dilutions were made of the blood and ground tissues and then incubated overnight at 37°C on LB agar plates; CFUs of bacteria were counted and calculated.

Bacteria preparation and fibrin clot experiment. *E. coli* and *E. faecalis* were identified by culturing contents of the ileum (Channing Laboratory, Brigham and Women's Hospital) and stored in LB media (Invitrogen) containing

20% glycerol (Sigma-Aldrich) at –80°C. For the infection models, *E. coli* and *E. faecalis* bacteria were grown in LB media for 24 hours at 37°C, and 1 ml bacteria was regrown in 9 ml LB media for 3 hours at 37°C. The bacteria were pelleted by centrifugation at 1,643 *g* for 10 minutes, washed in 10 ml PBS twice, and resuspended in 1 ml PBS. The bacteria were diluted in 1% bovine fibrinogen (Sigma-Aldrich) to produce a final bacterial concentration in the desired range (2×10^8 to 3×10^8 CFU/clot). Human thrombin (Sigma-Aldrich) was added at a final concentration of 2 U/ml, and the mixture was allowed to clot for 10 minutes (33). The bacterial concentration in the suspension and the clot was confirmed in each experiment by plating, overnight incubation at 37°C, and counting CFUs. To put fibrin clots into mice, anesthesia was administered in the same fashion as the CLP surgery. Using sterile conditions, the fibrin clot was placed within the peritoneal cavity via a 1.5-cm abdominal incision that was closed in layers with 6-0 surgical sutures (Harvard Apparatus). After surgery, the mice were injected with 1 ml of physiologic saline solution for fluid resuscitation.

Immunostaining. Aorta, ileum, and colon were fixed in methyl Carnoy solution at 4°C for 5 hours and then in 70% ethanol overnight; they were then embedded in paraffin. Sections were stained with H&E. To detect HO-1 expression, we stained sections with a polyclonal antibody to HO-1 (SPA-896, diluted 1:1,000; StressGen Biotechnologies) as described (31). Sections were also stained with a smooth muscle α-actin antibody (diluted 1:50; Sigma-Aldrich). Counterstaining of the sections was performed with methyl green.

FITC labeling of E. coli and E. faecalis and phagocytosis. After heat killing at 65°C for 25 minutes, *E. coli* and *E. faecalis* were incubated at a concentration of 6×10^9 to 8×10^9 CFU/ml with 0.2 mg FITC/ml (Sigma-Aldrich) in PBS for 1 hour at room temperature in the dark, as described (47). The bacteria were then washed 5 times with 1 ml PBS to remove free FITC, resuspended in 1 ml PBS, and stored at –80°C. 6×10^8 to 8×10^8 CFU nonlabeled or FITC-labeled *E. coli* or *E. faecalis* were injected into the peritoneum of WT C57BL/6 and Tg2 mice. After 24 hours, mouse peritoneal polymorphonuclear cells (PMNs) were isolated using 15 ml of DMEM cell culture media with 10% FBS, 10,000 U/ml penicillin, 10,000 mg/ml streptomycin, 29.2 mg/ml L-glutamine, and 10 U/ml heparin and then incubated for 1 hour at 37°C. Attached cells were washed with warm PBS 3 times and then treated with 0.2% Trypan blue for 1 minute at room temperature to quench extracellular fluorescence. The cells were washed twice, treated with a 5-mM EDTA solution containing PBS, scraped, and then centrifuged for 5 minutes at 2,147 *g*. The pellet was resuspended with 400 μl of 4% FBS and 0.009% sodium azide containing PBS. Total cells were counted, and 1×10^6 cells were scanned by flow cytometry (47).

Assessment of neutrophils and macrophages. Heat-killed *E. faecalis* bacteria were injected into the peritoneum of WT and Tg2 mice. After 24 hours, mouse peritoneal PMNs were isolated using 15 ml of DMEM cell culture media and incubated with 2 drops of ZAP-OGLOBIN II Lytic Reagent (Beckman Coulter Inc.) for 5 minutes at room temperature to lyse the red blood cells. Peritoneal PMNs were collected by centrifugation and total cells were counted using a Beckman Coulter counter. 1×10^6 cells from the peritoneal lavage were incubated with 1 μg of mouse CD16/CD32 (BD Biosciences — Pharmingen) antibody for 20 minutes at room temperature, washed with 1 ml staining buffer (4% FBS and 0.009% sodium azide containing PBS), and incubated with 100 μl staining buffer with 1 μg PE-conjugated mouse Ly-6G/Ly-6C (Gr-1 for neutrophils) and 1 μg FITC-conjugated mouse CD11c (for macrophages) antibodies for 1 hour at 4°C. Cells were then washed twice by 1 ml of staining buffer and the pellet resuspended with 400 μl of staining buffer. The cells were scanned by flow cytometry.

Systolic blood pressure. Systolic blood pressure was measured using a tail-cuff method as described previously (17).

Assessment of circulating leukocytes and cytokine levels. Blood was collected from heart and incubated with 2 drops of ZAP-OGLOBIN II Lytic Reagent (Beckman Coulter Inc.) for 5 minutes at room temperature to lyse the red blood cells. Total white blood cells (leukocytes) were counted using a Beckman Coulter counter (Beckman Coulter Inc.). Circulating levels of cytokines were assessed from blood serum by Linco Research Inc.

Real-time PCR and RT-PCR. Real-time PCR was performed as described previously (48). All PCRs were performed with the TaqMan kit (Applied Biosystems). Premade primers and probes were purchased from Applied Biosystems and assay IDs were as follows: mouse NOD2 (Mm00467543_m1) and mouse TLR4 (Mm00445274_m1). PCR cycling conditions were as follows: initial denaturation at 95°C for 10 minutes, followed by 40 cycles at 94°C for 30 seconds, 58°C for 15 seconds, and 72°C for 30 seconds and a 10-minute terminal incubation at 72°C. Expression of target genes was normalized to peptidyl-prolyl isomerase A (mPPIA) expression levels. For RT-PCR, primer sequences were as follows: hHO-1, 5′-TCTTCGCCCCTGTCTACTTCCC-3′ (forward) and 5′-TTGGTGTCATGGGTCAGCAGCT-3′ or 5′-CTGGGAGCCAGCATGCCTGCAT-3′ (reverse); and mouse β-actin, 5′-ATGGATGACGATATCGCTGAGC-3′ (forward) and 5′-CGTACATGGCTGGGGTGTTGAA-3′ (reverse).

Statistics. Data are expressed as mean ± SEM. For comparisons between 2 groups, we used 2-tailed unpaired Student's *t* test. For comparison among more than 2 groups and multiple comparisons, we used an ANOVA test. Analysis of bacterial cultures were made by nonparametric Mann-Whitney *U* analysis. Comparisons of mortality were made by analyzing Kaplan-Meier survival curves, and then log-rank test was used to assess for differences in survival. The number of samples per group (*n*) is specified in Results or in the figure legend. Statistical significance was accepted at $P < 0.05$.

Acknowledgments

We are thankful to S.-F. Yet, M.D. Layne, D. Soybel, A. Mitsialis, and S. Kourembanas for advice and helpful suggestions; A.M. Houghton and L.A. Marconcini for help with bacterial cultures; M. Baron, M. Delaney, and A. Onderdonk for identification of the bowel bacterial flora; S. Srisuma and T. Mariani for real-time PCR; R. Takamiya for help with HO-$1^{-/-}$ mice; and L. Kobzik for review of the pathology slides. This work was supported in part by grants HL60788, AI061246, and GM53249 from the NIH (to M.A. Perrella).

Received for publication May 18, 2007, and accepted in revised form October 3, 2007.

Address correspondence to: Mark A. Perrella, Division of Pulmonary and Critical Care Medicine, Brigham and Women's Hospital, 75 Francis Street, Boston, Massachusetts 02115, USA. Phone: (617) 732-6809; Fax: (617) 582-6148; E-mail: mperrella@rics.bwh.harvard.edu.

1. Hotchkiss, R.S., and Karl, I.E. 2003. The pathophysiology and treatment of sepsis. *N. Engl. J. Med.* **348**:138–150.
2. Baron, R.M., Baron, M.J., and Perrella, M.A. 2006. Pathobiology of sepsis. Are we still asking the same questions? *Am. J. Respir. Cell Mol. Biol.* **34**:129–134.
3. Levy, M.M., et al. 2003. 2001 SCCM/ESICM/ACCP/ATS/SIS International Sepsis Definitions Conference. *Crit. Care Med.* **31**:1250–1256.
4. Bone, R.C., Grodzin, C.J., and Balk, R.A. 1997. Sepsis: A new hypothesis for pathogenesis of the disease process. *Chest.* **112**:235–243.
5. Pinsky, M.R. 2001. Sepsis: a pro- and anti-inflammatory disequilibrium syndrome. *Contrib. Nephrol.* **132**:354–366.
6. Rivers, E., et al. 2001. Early goal-directed therapy in the treatment of severe sepsis and septic shock. *N. Engl. J. Med.* **345**:1368–1377.
7. Rivers, E.P., McIntyre, L., Morro, D.C., and Rivers, K.K. 2005. Early and innovative interventions for severe sepsis and septic shock: taking advantage of a window of opportunity. *CMAJ.* **173**:1054–1065.
8. Bernard, G., et al. 2001. Efficacy and safety of recombinant human activated protein C for severe sepsis. *N. Engl. J. Med.* **344**:699–709.
9. Annane, D., Bellissant, E., and Cavaillon, J.M. 2005. Septic shock. *Lancet.* **365**:63–78.

10. Riedemann, N.C., Guo, R.-F., and Ward, P.A. 2003. Novel strategies for the treatment of sepsis. *Nat. Med.* **9**:517–524.
11. Strober, W., Murray, P.J., Kitani, A., and Watanabe, T. 2006. Signalling pathways and molecular interactions of NOD1 and NOD2. *Nat. Rev. Immunol.* **6**:9–20.
12. Takeda, K., and Akira, S. 2005. Toll-like receptors in innate immunity. *Int. Immunol.* **17**:1–14.
13. Elphick, D.A., and Mahida, Y.R. 2005. Paneth cells: their role in innate immunity and inflammatory disease. *Gut.* **54**:1802–1809.
14. Kobayashi, K.S., et al. 2005. Nod2-dependent regulation of innate and adaptive immunity in the intestinal tract. *Science.* **307**:731–734.
15. Poss, K.D., and Tonegawa, S. 1997. Reduced stress defense in heme oxygenase 1-deficient cells. *Proc. Natl. Acad. Sci. U. S. A.* **94**:10925–10930.
16. Yet, S.-F., et al. 1999. Hypoxia induces severe right ventricular dilatation and infarction in heme oxygenase-1 null mice. *J. Clin. Invest.* **103**:R23–R29.
17. Wiesel, P., et al. 2000. Endotoxin-induced mortality is related to increased oxidative stress and end-organ dysfunction, not refractory hypotension, in heme oxygenase-1 deficient mice. *Circulation.* **102**:3015–3022.
18. Abraham, N.G., and Kappas, A. 2005. Heme oxygenase and the cardiovascular-renal system. *Free Radic. Biol. Med.* **39**:1–25.
19. Maines, M.D., and Gibbs, P.E.M. 2005. 30 years of heme oxygenase: From a "molecular wrecking ball" to a "mesmerizing" trigger of cellular events. *Biochem. Biophys. Res. Commun.* **338**:568–577.
20. Ryter, S.W., Alam, J., and Choi, A.M.K. 2006. Heme oxygenase-1/carbon monoxide: From basic science to therapeutic implications. *Physiol. Rev.* **86**:583–650.
21. Stocker, R., Yamamoto, Y., McDonagh, A.F., Glazer, A.N., and Ames, B.N. 1987. Bilirubin is an antioxidant of possible physiological importance. *Science.* **235**:1043–1046.
22. Sarady-Andrews, J.K., et al. 2005. Biliverdin administration protects against endotoxin-induced acute lung injury in rats. *Am. J. Physiol. Lung Cell Mol. Physiol.* **289**:L1131–L1137.
23. Balla, G., et al. 1992. Ferritin: a cytoprotective antioxidant strategem of endothelium. *J. Biol. Chem.* **267**:18148–18153.
24. Otterbein, L.E., et al. 2000. Carbon monoxide has anti-inflammatory effects involving the mitogen-activated protein kinase pathway. *Nat. Med.* **6**:422–428.
25. Morse, D., et al. 2003. Suppression of inflammatory cytokine production by carbon monoxide involves the JNK pathway and AP-1. *J. Biol. Chem.* **278**:36993–36998.
26. Mazzola, S., et al. 2005. Carbon monoxide pretreatment prevents respiratory derangement and ameliorates hyperacute endotoxic shock in pigs. *FASEB J.* **19**:2045–2047.
27. Foresti, R., et al. 2005. Reviewing the use of carbon monoxide-releasing molecules (CO-RMs) in biology: implications in endotoxin-mediated vascular dysfunction. *Cell. Mol. Biol.* **51**:409–423.
28. Overhaus, M., et al. 2006. Biliverdin protects against polymicrobial sepsis by modulating inflammatory mediators. *Am. J. Physiol. (Gastrointest. Liver Physiol.)* **290**:G695–G703.
29. Layne, M.D., et al. 2002. Characterization of the mouse aortic carboxypeptidase-like protein promoter reveals activity in differentiated and dedifferentiated vascular smooth muscle cells. *Circ. Res.* **90**:728–736.
30. Yet, S.-F., et al. 2001. Cardiac specific expression of heme oxygenase-1 protects against ischemia and reperfusion injury in transgenic mice. *Circ. Res.* **89**:168–173.
31. Yet, S.-F., Melo, L.G., Layne, M.D., and Perrella, M.A. 2002. Heme oxygenase-1 in the regulation of inflammation and oxidative damage. *Methods Enzymol.* **353**:163–176.
32. Imai, T., et al. 2001. Vascular smooth muscle cell-directed overexpression of heme oxygenase-1 elevates blood pressure through attenuation of nitric oxide-induced vasodilation in mice. *Circ. Res.* **89**:55–62.
33. Matute-Bello, G., et al. 2001. Septic shock and acute lung injury in rabbits with peritonitis. *Am. J. Respir. Crit. Care Med.* **163**:234–243.
34. Minamino, T., et al. 2001. Targeted expression of heme oxygenase-1 prevents the pulmonary inflammatory and vascular responses to hypoxia. *Proc. Natl. Acad. Sci. U. S. A.* **98**:8798–8803.
35. Stone, R. 1994. Search for sepsis drugs goes on despite past failures. *Science.* **264**:365–367.
36. Angus, D.C., et al. 2001. Epidemiology of severe sepsis in the United States: analysis of incidence, outcome, and associated costs of care. *Crit. Care Med.* **29**:1303–1310.
37. Hotchkiss, R.S., et al. 1999. Apoptotic cell death in patients with sepsis, shock, and multiple organ dysfunction. *Crit. Care Med.* **27**:1230–1251.
38. Otterbein, L.E., May, A., and Chin, B.Y. 2005. Carbon monoxide increases macrophage bacterial clearance through Toll-like receptor (TLR)4 expression. *Cell. Mol. Biol.* **51**:433–440.
39. Nakahira, K., et al. 2006. Carbon monoxide differentially inhibits TLR signaling pathways by regulating ROS-induced trafficking of TLRs to lipid rafts. *J. Exp. Med.* **203**:2377–2389.
40. Cario, E. 2005. Bacterial interactions with cells of the intestinal mucosa: Toll-like receptors and NOD2. *Gut.* **54**:1182–1193.
41. Exner, M., Minar, E., Wagner, O., and Schillinger, M. 2004. The role of heme oxygenase-1 promoter polymorphisms in human disease. *Free Radic. Biol. Med.* **37**:1097–1104.
42. Yachie, A., et al. 1999. Oxidative stress causes enhanced endothelial cell injury in human heme oxygenase-1 deficiency. *J. Clin. Invest.* **103**:129–135.
43. Wang, P., Ba, Z.F., and Chaudry, I.H. 1992. Hepatocellular dysfunction persists during early sepsis despite increased volume of crystalloid resuscitation. *J. Trauma.* **32**:389–396.
44. Motterlini, R., et al. 2002. Carbon monoxide-releasing molecules. Characterization of biochemical and vascular activities. *Circ. Res.* **90**:e17–e24.
45. Baker, C.C., Chaudry, I.H., Gaines, H.O., and Baue, A.E. 1983. Evaluation of factors affecting mortality rate after sepsis in a murine cecal ligation and puncture model. *Surgery.* **94**:331–335.
46. Godshall, C.J., Scott, M.J., Peyton, J.C., Gardner, S.A., and Cheadle, W.G. 2002. Genetic background determines susceptibility during murine septic peritonitis. *J. Surg. Res.* **102**:45–49.
47. Henneke, P., et al. 2002. Cellular activation, phagocytosis, and bactericidal activity against group B streptococcus involve parallel myeloid differentiation factor 88-dependent and independent signaling pathways. *J. Immunol.* **169**:3970–3977.
48. Arikan, M.C., Shapiro, S.D., and Mariani, T.J. 2005. Induction of macrophage elastase (MMP-12) gene expression by statins. *J. Cell Physiol.* **204**:139–145.